Optimal Power Flow of Radial Networks and its Variations: A Sequential Convex Optimization Approach

Wei Wei, *Member, IEEE,* Jianhui Wang, *Senior Member, IEEE,* Na Li, *Member, IEEE*, and Shengwei Mei, *Fellow, IEEE*

***Abstract*—This paper proposes a sequential convex optimization method to solve broader classes of optimal power flow (OPF) problems over radial networks. The non-convex branch power flow equation is decomposed as a second-order cone inequality and a non-convex constraint involving the difference of two convex functions. Provided with an initial solution offered by an inexact second-order cone programming relaxation model, this approach solves a sequence of convexified penalization problems, where concave terms are approximated by linear functions and updated in each iteration. It could recover a feasible power flow solution, which usually appears to be very close, if not equal, to the global optimal one. Two variations of the OPF problem, in which non-cost related objectives are optimized subject to power flow constraints and the convex relaxation is generally inexact, are elaborated in detail. One is the maximum loadability problem, which is formulated as a special OPF problem that seeks the maximal distance to the boundary of power flow insolvability. The proposed method is shown to outperform commercial nonlinear solvers in terms of robustness and efficiency. The other is the bi-objective OPF problem. A non-parametric scalarization model is suggested, and is further reformulated as an extended OPF problem by convexifying the objective function. It provides a single trade-off solution without any subjective preference. The proposed computation framework also helps retrieve the Pareto front of the bi-objective OPF via the ε-constraint method or the normal boundary intersection method. This paper also discusses extensions for OPF problems over meshed networks based on the semidefinite programming relaxation method.**

***Index Terms*—bi-objective optimization, convex optimization, difference-of-convex programming, maximum loadability, optimal power flow, radial network**

NOMENCLATURE

The major symbols and notations used throughout the paper are defined below for quick reference. Others are clarified after their first appearance as required.

A. Sets

B	Set of buses except the slack bus.
$c(i)$	Child buses of bus i, empty set for terminal buses.
L	Set of lines.

B. Parameters

a_i^g, b_i^g	Coefficients of the production cost function.
p_i^d, q_i^d	Fixed active and reactive power demand.
p_i^n, p_i^m	Active generation limits at bus i.
q_i^n, q_i^m	Reactive generation limits at bus i.
r_{ij}^l, x_{ij}^l	Resistance and reactance of line l.
S_l	Apparent power flow capacity of line l.
U_i^r	Reference value of square voltage magnitude.
U_i^n, U_i^m	Bounds of square voltage magnitudes.
z_{ij}^l	Impedance of line l, $(z_{ij}^l)^2 = (r_{ij}^l)^2 + (x_{ij}^l)^2$.
ξ	Electricity price at the slack bus.

C. Variables

I_{ij}^l	Square magnitude of current in line l.
p_i^g	Active power generation at bus i.
P_{ij}^l	Active power flow in line l.
q_i^g	Reactive power generation at bus i.
Q_{ij}^l	Reactive power flow in line l.
t_1, t_2, t_b	Convexification variables used in bi-objective OPF problems.
U_i	Square voltage magnitude at bus i.
η	Loadability index.

D. Abbreviations

BO-OPF	Bi-objective optimal power flow
BIM	Bus injection model
BFM	Branch flow model
CCP	Convex-concave procedure
DC	Difference-of-convex
DCP	DC programming
DN	Distribution network
FRP	Feasibility recovery procedure
MLA	Maximal loadability
NBI	Normal boundary intersection
NLP	Nonlinear programming
ORP	Optimality recovery procedure
OPF	Optimal power flow
SDP	Semidefinite programming

The work of W. Wei and S. Mei is supported by the National Natural Science Foundation of China under grant 51621065. The work of J. Wang is supported by the U.S. Department of Energy (DOE)'s Office of Electricity Delivery and Energy Reliability under contract DE-OE0000839. The work of N. Li is supported by NSF CAREER under grant 1553407. *Corresponding to: Wei Wei.*

W. Wei and S. Mei are with the State Key Laboratory of Control and Simulation of Power Systems and Generation Equipments, Department of Electrical Engineering, Tsinghua University, Beijing, 100084, China. (e-mail: wei-wei04@mails.tsinghua.edu.cn, meishengwei@mail.tsinghua.edu.cn).

J. Wang is with the Department of Electrical Engineering at Southern Methodist University, Dallas, TX 75205 USA and the Energy Systems Division at Argonne National Laboratory, Argonne, IL 60439 USA (e-mail: jianhui.wang@ieee.org).

N. Li is with the School of Engineering and Applied Sciences, Harvard University, Cambridge, MA 02138 USA. (e-mail: nali@seas.harvard.edu).

SOC	Second-order cone
SOCP	Second-order cone program

E. Other Notations

A tuple (l, i, j) is used to denote a line $l \in L$ together with its head bus $i \in B$ and tail bus $j \in B$. Vectors $p^g = [p_i^g], \forall i$, $q^g = [q_i^g], \forall i$, $U = [U_i], \forall i$, $P = [P_{ij}^l], \forall l$, $Q = [Q_{ij}^l], \forall l$, $I = [I_{ij}^l], \forall l$. Vector $x = [p^g; q^g; U; I; P; Q]$ is the decision variable of the OPF problem in compact form, $t = [t_1, t_2, t_b]^T$. Convex functions $f_l(x)$ and $g_l(x)$ are used to represent branch flow equality of line l in a DC format, $\epsilon_l, \forall l$ stands for the line-wise relaxation gap, $\text{Gap}_r(x)$ is the aggregated relaxation gap for the system.

I. Introduction

THE alternating current optimal power flow (OPF for short), a fundamental issue of power system steady-state operation, determines the most effective utilization of generation assets subject to necessary component and network operating constraints. Traditional OPF problem are based on either the bus injection model (BIM) [1] or the branch flow model (BFM) [2]–[4]. Both models can be formulated as non-convex quadratically constrained quadratic programs. In theory, the global optimal solution cannot be found in polynomial time. OPF problems can be solved locally by a number of general-purpose nonlinear programming (NLP) techniques. Up-to-date surveys of available algorithms can be found in [5]–[7] (deterministic ones) and [8] (non-deterministic ones), with different preferences or tradeoffs on optimality and computational efficiency.

In view of the potential economic benefit, there has been growing interest on computing the global OPF solution. In recent years, important progresses have been reported based on convex relaxation methods, such as semidefinite programming (SDP) relaxation [9], [10], second-order cone programming (SOCP) relaxation [11] (for BIMs) [12] (for BFMs), moment relaxation [13]–[15], and convex quadratic relaxation [16]. Convex relaxation models could provide a lower bound for the objective value at optimum, and may even globally solve an OPF problem if the relaxation is exact.

From a theoretical point of view, establishing sufficient conditions that guarantee an exact convex relaxation (ex-ante) has received substantial attention. A spate of such conditions have been reported in literature. The pioneer work in [10] finds that the SDP relaxation will be exact for several IEEE benchmark systems after adding a small resistance to every purely inductive transformer branch, and opens up a promising research direction in OPF studies. It is proven in [17], [18] that the SDP relaxation will be exact with allowance of load over-satisfaction and utilization of virtual phase shifters. For distribution networks operated with tree topology, it is shown in [12] that if the objective function is convex, strictly increasing in line losses, non-increasing in loads, and independent of complex line flows, then the SOCP relaxation will be exact provided that the original OPF is feasible. Geometry of the power flow injection region is studied in [19], [20]. It is revealed that the Pareto front of nodal power injection region remains unchanged by taking the convex hull under certain conditions, which implies that when the objective function is convex and strictly increasing in power injection, the convex relaxation model is very likely to be exact. This geometry property has been extended to generalized network flow problem over an arbitrary network described by a graph [21]. It is demonstrated in [22] that if: i) the objective function is strictly increasing in active power injection, ii) there is no reverse flow, and iii) the upper bounds on voltage magnitudes are not binding, the SOCP relaxation will be exact. Further conditions on system parameters which admit provable exactness guarantee are suggested in [23]. It is revealed in [24] that if there is no simultaneous reverse active and reactive power flows, the SOCP relaxation will be exact.

As we can observe from studies mentioned above, the exactness of relaxed OPF models for general meshed networks largely depends on the choice of the objective function and may be sensitive to system data. If the relaxation is not exact, its solution is not feasible for the original OPF problem. In such circumstance, one possible remedy is to improve the relaxation via valid inequalities [11], [25]. Valid inequalities do enhance the tightness of relaxation and reduce the optimality gap, but still fail to recover the optimal solution for the original OPF problem in many cases. In the SDP relaxation model, exactness is achieved when the symmetric matrix variable has a rank-1 solution. In order to enforce a rank-1 matrix optimizer which contains a physically meaningful power flow solution, it is proposed to append rank-related penalty terms in the objective function [26]–[28]. Computational results show that the rank penalty method is very inspiring. Another approach to construct a tight convex relaxation is to employ the moment method from polynomial optimization, which solves a sequence of SDPs with increasing problem sizes, as discussed in [13]–[15]. In theory, the global OPF solution can be recovered with the order of moment relaxation approaching infinity. However, this method may suffer from a high computational overhead due to the dramatic growing SDP sizes when the order of moment relaxation becomes higher. There are research efforts on globally solving the OPF problem by using branch-and-bound type methods, such as those in [29], [30], while abandoning a polynomial-time complexity guarantee.

Although the convex relaxation is proved to be exact for radial networks under relative mild conditions, in practice, there are still a lot of factors that could challenge these conditions, especially those on the objective function. In traditional cost minimization formulations, if the cost function is not strictly increasing in the nodal active power injection (this situation is not rare because renewable units can have zero production costs), the exactness may no longer be guaranteed. Moreover, if non-cost goals are considered for optimization, the objective function may appear to be non-convex and non-monotonic, which also jeopardizes the exactness. For example, system operation associated with loadability maximization and voltage regulation can be cast as special classes of OPF problems with non-cost oriented objectives, in which the convex relaxation is generally inexact. Special cases of inexact SDP and SOCP relaxation in voltage stability problems have been reported in [31], [32]. Finally, if more than one optimization targets are

incorporated, and a weighted-sum objective is under investigation, the convex relaxation could be inexact, even if only one objective is non-monotonic or non-convex.

In contrast to preceding studies which aim to explore a provable exactness guarantee, this paper develops a versatile computational framework for broader classes of OPF problems over radial networks based on the difference-of-convex (DC) programming (DCP) approach. DCP belongs to the class of non-convex optimization, whose objective and constraints involve non-convex functions expressed by the difference of two convex functions. This type of mathematic program has been studied for several decades. Theoretical foundations of DCP and some overviews can be found in [33]–[35]. Due to its non-convexity, solving DCPs globally often proves slow in practice [36]. A local algorithm, called the convex-concave procedure (CCP), is suggested in [36]. Compared with prevalent algorithms for DCPs, CCP does not require conjugate function, and is often more robust than standard NLP methods. The success of CCP inspires its application in OPF problems. The contributions of this paper are threefold.

1) A sequential SOCP method for the OPF problem of radial networks based on BFM in [2]–[4] and CCP in [36] (CCP-OPF for short), which relaxes most assumptions for ensuring exactness and leverages the computational superiority of SOCPs. The nonlinear branch power flow equality is decomposed as a rotated SOC constraint and a DC inequality. Starting from an initial (infeasible) solution offered by an inexact SOCP relaxation model, a sequence of convexified penalization problems are solved, where the concave part is replaced by its linear approximation and updated in each iteration. A feasible solution can be quickly recovered, which usually appears to be very close, if not equal, to the global optimal one. Convergence is guaranteed by the property of DCP and the existence of an exact penalty parameter. The advantage of CCP-OPF is apparent in three aspects. First, it relies solely on solving SOCPs. The interior point method (IPM) is proved to be efficient for this task [37]. Second, it removes the need of an initial guess, which is required by the majority of prevalent local NLP algorithms, and the need of an ex-ante exactness guarantee, which is desired by existing convex relaxation methods. Finally, it reduces the computation overhead of branch-and-bound type methods, and provides a high-quality solution within reasonable efforts. In summary, CCP-OPF greatly enhances our ability to solve OPF problems with various objectives.
2) A systematic approach for the bi-objective OPF (BO-OPF) problem. A non-parametric scalarization model for BO-OPF is suggested. Its objective function can be convexified through introducing auxiliary variables and convex constraints. Based on this fact, BO-OPF can be cast as an extended OPF problem, which can be solved by CCP-OPF. It procures a single Pareto optimal solution which compromise both objectives without any subjective parameter. The proposed CCP-OPF also help retrieve the Pareto front via the ε-constraint method (with some delicately sampled values of ε) or the normal boundary intersection (NBI) method.
3) Applying CCP-OPF to the maximum loadability (MLA) problem, which is formulated as a special OPF problem that optimizes the distance from a specified operating point to the boundary of power flow insolvability. Traditional convex relaxation is shown to be inexact for this class of problem [31], [32], while CCP-OPF successfully solves all testing instances, and outperforms commercial NLP solvers in terms of robustness and efficiency.

The rest of this paper is organized as follows. The mathematical formulation of BFM based OPF problem and CCP-OPF method are presented in Section II, and then an extension to meshed networks is suggested based on a DC expression of the matrix rank-1 constraint. As a direct application, MLA problem is discussed in Section III. BO-OPF problem is studied in Section IV, including technical details on the non-parametric scalarization model and its convexification form, as well as implementations of the ε-constrained method and NBI method. Case studies are provided in Sections II-IV. Finally, conclusions are summarized in Section V.

II. OPF Problem

A. Branch Flow Model

The typical connection of branches in a radial power grid is illustrated in Fig. 1. The steady-state network power flow status can be described by BFM proposed in [2]–[4] as

$$P_{ij}^l + p_j^g - r_{ij}^l I_{ij}^l = \sum_{k\in\pi(j)} P_{jk}^l + p_j^d,\ \forall j \in B \tag{1}$$

$$Q_{ij}^l + q_j^g - x_{ij}^l I_{ij}^l = \sum_{k\in\pi(j)} Q_{jk}^l + q_j^d,\ \forall j \in B \tag{2}$$

$$U_j = U_i - 2(r_{ij}^l P_{ij}^l + x_{ij}^l Q_{ij}^l) + (z_{ij}^l)^2 I_{ij}^l,\ \forall l \in L \tag{3}$$

$$I_{ij}^l U_i = (P_{ij}^l)^2 + (Q_{ij}^l)^2,\ \forall l \in L \tag{4}$$

where constraints (1)-(2) are nodal active power and reactive power balancing conditions; According to the reference direction of power flow shown in Fig. 1, the left-hand (right-hand) side gathers total active and reactive power injected (withdrawn) in (from) bus j; (3) describes forward voltage drop on each line; (4) defines apparent power flow injection at the head bus of each line. The square voltage magnitude U_0 at the slack bus is a constant. It is proved in [17] that BFM (1)-(4) and traditional BIM in rectangle coordinate produce the same voltage magnitude and line power flow in OPF applications for radial networks. BFM is more straightforward for distribution networks (DNs), because they are intentionally operated with tree topologies. More importantly, the voltage magnitude plays a crucial role in voltage instability, a major threat to DN operating security, and thus is closely monitored. The voltage angle in DN is difficult to measure and receives less attention, as angle instability scarcely happens in DNs. In contrast to BIM in which power balancing conditions render non-convex quadratic equalities, (1)-(2) in BFM are linear, and non-convexity only appears in branch flow equality (4).

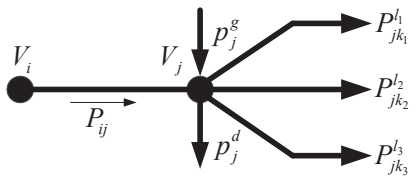

Fig. 1. Typical connection of a branch in DN.

B. OPF as DCP

Without loss of generality, the compact form of OPF problem can be expressed as follows

$$\min_x \{F(x) : \text{Cons-PF, Cons-BD}\} \tag{5}$$

where aggregated variable x has been defined in Nomenclature, Cons-PF consists of power flow constraints (1)-(4), and Cons-BD includes the following operating security boundary constraints

$$p_i^n \le p_i^g \le p_i^m, q_i^n \le q_i^g \le q_i^m, U_i^n \le U_i \le U_i^m, \forall i \in B$$

$$P_{ij}^l \ge 0,\ Q_{ij}^l \ge 0,\ \sqrt{(P_{ij}^l)^2 + (Q_{ij}^l)^2} \le S_l,\ \forall l \in L$$

The first set of inequalities imposes admissible intervals on nodal injection power and bus voltage; owing to relay protection and security considerations, the second set of inequalities prevents reverse power flow and over flow in each line. In fact, in some active DNs and micro-grids with high share of renewables, reserve power flow is allowed, which might influence the exactness of convex relaxation (see conditions in [22]). However, removing flow direction restriction brings little injury on the proposed method, because its aim is to tackle inexactness introduced by convex relaxation. Without loss of generality, objective function $F(x)$ is assumed to be convex without further requirements on monotonicity. Extensions for non-convex objectives is allowed and will be discussed later. Typical objectives used in this paper are summarized below.

1) Production cost

$$F_C = \sum_{i \in B} \left[a_i (p_i^g)^2 + b_i p_i^g\right] + \xi \sum_{j \in \pi(0)} P_{0j}^l \tag{6}$$

The first part is the fuel cost of generators. P_{0j}^l represents the amount of active power delivered through line l connected to the slack bus, hence the second term is the energy transaction cost with the main grid.

2) Voltage profile. In power system operation, one task is to maintain the voltage magnitude at every bus close to its reference value, yielding the following objective

$$F_V = \sum_i (U_i - U_i^r)^2 \tag{7}$$

Although F_V is convex, it is not monotonic. Thus convex relaxation for pertinent OPF problems is generally inexact if F_V appears in their objective(s).

OPF problem (5) is non-convex. In what follows, quadratic equality (4) will be arranged as a particular format involving the difference of two convex functions, which is called a DC formulation, or DC constraint, or DC inequality. These terms will be used interchangeably in this paper. Constraints or inequalities that admit a DC formulation are called DC-representable. DC constraints are non-convex and do not alter problem complexity. Nevertheless, the special structure of DC inequality helps develop algorithms with good convergence properties based on convex optimization.

Define the following convex quadratic functions

$$f_l(x) = (U_i + I_{ij}^l)^2,\ \forall l \in L$$

$$g_l(x) = (U_i - I_{ij}^l)^2 + (2P_{ij}^l)^2 + (2Q_{ij}^l)^2,\ \forall l \in L$$

equality (4) can be replaced by two opposite inequalities

$$f_l(x) - g_l(x) \ge 0,\ \forall l \in L \tag{8}$$

$$f_l(x) - g_l(x) \le 0,\ \forall l \in L \tag{9}$$

The former one in (8) is in fact an SOC constraint, whose canonical form is given by

$$\left\| \begin{array}{c} 2P_{ij}^l \\ 2Q_{ij}^l \\ I_{ij}^l - U_i \end{array} \right\|_2 \le I_{ij}^l + U_i,\ \forall l \in L \tag{10}$$

while the latter one in (9) is a DC inequality. (8) and (9) constitute a DC formulation of branch flow inequality (4).

Define the convex power flow feasible set

$$X = \{\ x \mid (1) - (3),\ (10),\ \text{Cons-BD}\ \}$$

which consists of linear and SOC constraints. OPF problem (5) can be expressed in the following compact DCP form

$$\min\{F(x) : x \in X,\ (9)\} \tag{11}$$

where (9) is a DC constraint. The classical SOCP relaxation model in [12] neglects (9), resulting in an SOCP

$$\text{OPF-Cr} \quad \min\{F(x) : x \in X\} \tag{12}$$

If the solution of (12) naturally meets (9), the relaxation is said to be exact. At the same time, the solution is globally optimal. Otherwise, the relaxation is not exact, and the solution is infeasible in (5). An infeasible solution cannot be deployed in practice.

C. CCP-OPF Method

CCP-OPF method consists of three major steps: an initial SOCP relaxation, a feasibility recovery procedure (FRP), and an optimality recovery procedure (ORP). The first step refers to the well-known SOCP relaxation. If the relaxation gap is not small enough, the infeasible solution is passed to FRP, which produces a feasible power flow solution in the second step. Finally, an adjacent optimal solution is refined by ORP in the third step, in case the solution offered by FRP is not optimal. The flowchart of CCP-OPF is shown in Algorithm 1.

In FRP, DC-inequality (9) which is ignored in the initial SOCP relaxation is convexified by linearizing concave terms and adding slack variables. Moreover, the total constraint violation is penalized in the objective function. The flowchart of FRP is summarized in Algorithm 2. Its convergence is explained as follows.

Algorithm 1 : CCP-OPF

1: Solve OPF-Cr (12), the optimal solution is x^*. Evaluate the relaxation gap at x^* as

$$\text{Gap}_r(x^*) = \sum\nolimits_l r_{ij}^l \left[I_{ij}^{l*} U_i^* - (P_{ij}^{l*})^2 - (Q_{ij}^{l^*})^2 \right] \quad (13)$$

If $\text{Gap}_r(x^*) \leq \varepsilon$, where ε is a pre-specified tolerance, terminate and report the optimal solution x^* and the optimal value v^*.

2: Perform FRP (summarized in Algorithm 2) with initial point x^*, and find a feasible power flow solution x^F.

3: Perform ORP (solve OPF (5) in its original nonlinear form via local NLP methods) with initial point x^F, and refine an optimal solution x^S.

Algorithm 2 : FRP

1: Set an initial penalty coefficient $\rho^1 > 0$, a penalty growth rate parameter $\tau > 1$, and a penalty upper bound ρ_M. Let the iteration index $k = 1$, and the initial point $x^1 = x^*$ (passed from OPF-Cr).

2: Form linear approximation of $g_l(x)$ at x^k

$$\bar{g}_l(x, x^k) = g_l(x^k) + \nabla g_l(x^k)^T (x - x^k), \forall l \in L \quad (14)$$

and solve the following penalized problem

$$\begin{aligned} \min \quad & v(x,s) = F(x) + \rho^k \sum\nolimits_l s_l \\ \text{s.t.} \quad & x \in X,\ s_l \geq 0,\ \forall l \in L \\ & f_l(x) - \bar{g}_l(x, x^k) \leq s_l,\ \forall l \in L \end{aligned} \quad (15)$$

the optimal solution is (x^{k+1}, s^{k+1}), and the optimal value is v^{k+1}.

3: Evaluate the relaxation gap at x^{k+1}, if $\text{Gap}_r(x^{k+1}) \leq \varepsilon$, terminate, and report $x^F = x^{k+1}$; otherwise; update $\rho^{k+1} = \min\{\tau\rho^k, \rho_M\}$, $k \leftarrow k+1$, and go to step 2.

If $\text{Gap}(x^k)$ becomes small enough before ρ^k reaches ρ_M, convergence has already been guaranteed. Otherwise, the penalty parameter ρ^k will be fixed at ρ_M and the objective function of (15) does not change in the subsequent iterations. Next we consider the latter case, and demonstrate the monotonicity of objective value sequence $\{v(x^k, s^k)\}_k$ generated in step 2 when $k > \log_\tau(\rho_M/\rho^1)$. Two basic facts on functions $\bar{g}_l(x, x^k)$ and $g_l(x)$ play an important role in the discussion.

F1: According to (14), $\bar{g}_l(x^k, x^k) = g_l(x^k)$.

F2: According to the property of convex functions, for an arbitrarily given x^k, $g_l(x) \geq \bar{g}_l(x, x^k), \forall x$ holds.

The relaxation gap of line l in iteration k is defined by

$$\epsilon_l^k = f_l(x^k) - g_l(x^k)$$

and vector $\epsilon^k = [\epsilon_l^k], \forall l$ will be frequently used.

The definition of ϵ_l^k and F1 implies that $f_l(x^k) - g_l(x^k) = f_l(x^k) - \bar{g}_l(x^k, x^k) \leq \epsilon^k, \forall l$ is satisfied, therefore (x^k, ϵ^k) is a feasible solution of (15) in iteration k. Denote by (x^{k+1}, s^{k+1}) the optimal solution of (15) in iteration k, we can assert that

$$v(x^{k+1}, s^{k+1}) \leq v(x^k, \epsilon^k) \quad (16)$$

because $v(x, s)$ is minimized in that iteration. The objective at optimal solution (x^{k+1}, s^{k+1}) deserves a value no greater than that corresponds to a feasible solution (x^k, ϵ^k). In addition, according to F2, we have

$$\begin{aligned} \epsilon_l^{k+1} &= f_l(x^{k+1}) - g_l(x^{k+1}) \\ &\leq f_l(x^{k+1}) - \bar{g}_l(x^{k+1}, x^k) \leq s_l^{k+1},\ \forall l \end{aligned}$$

The last inequality is a constraint of (15) which the optimal solution (x^{k+1}, s^{k+1}) must satisfy. For the same reason, $\epsilon_l^k \leq s_l^k, \forall l$. Because $v(x, s)$ is strictly increasing in its second input, we arrive at

$$v(x^k, \epsilon^k) \leq v(x^k, s^k) \quad (17)$$

(16) and (17) conclude the following monotonic relation

$$v(x^{k+1}, s^{k+1}) \leq v(x^k, s^k) \quad (18)$$

Strict inequality holds in (18) if one or more of the following conditions are met:

1) $v(x^{k+1}, s^{k+1}) < v(x^k, \epsilon^k)$
2) $U_i^{k+1} - I_{ij}^{l(k+1)} \neq U_i^k - I_{ij}^{lk}$
3) $P_{ij}^{l(k+1)} \neq P_{ij}^{lk}$
4) $Q_{ij}^{l(k+1)} \neq Q_{ij}^{lk}$

which is generally true in practical OPF problems. Therefore, the sequence $\{v(x^k, s^k)\}_k$ is decreasing. (18) indicates that as long as the convergence criterion is not met, $v(x, s)$ can be strictly improved in the next iteration. Since v has a finite optimum, Algorithm 2 converges with $v(x^k, s^k)$ approaching constant values. Because OPF problems with network losses usually has a unique optimal solution [20], there is a one-to-one mapping between optimal solutions and optimal values, so (x^k, s^k) also converges.

To ensure slack variables s^k converge to 0, the value of ρ_M should be greater than the exact penalty parameter ρ_M^* [36]. According to the exact penalty function theory [38], [39], if OPF problem (11) is feasible and certain constraint qualification holds, there will be a finite penalty parameter ρ_M^*, such that for any $\rho^* \geq \rho_M^*$, the following penalized problem

$$\min_{x \in X}\ F(x) + \rho^* \sum\nolimits_l [f_l(x) - g_l(x)]$$

has the same optimal solution as (11).

It should be mentioned that if ρ_M is not big enough, problem (15) may give $x^{k+1} = x^k$ before s^k approaches 0 due to the lack of enough penalty. In such circumstance, v^k (ϵ^k) cannot be improved (reduced) any more, and Algorithm 2 may fail to converge.

Owing to the convergence criterion used in Algorithm 2, the solution x^F offered by FRP may not be optimal. Thus we incorporate ORP to refine an adjacent optimal solution. Any traditional OPF methods or NLP solvers are eligible for this task, such as the interior point method [40]–[42], and the sequential quadratic programming method [43]–[45]. Nonetheless, if we delicately choose penalty parameters in Algorithm 2, it will directly procure a solution that is very close to, if not equal, to the global optimal one. Additional observations are given below.

1) From our numerical experiences, to recover the global optimal solution, it is very useful to use a small initial

value of ρ^1. The reason is: first, temporarily constraint violations may allow x^k move to a more favorable region where the optimal solution stays; second, light penalty does not cause dramatic change of optimal solutions in two succussive iterations. Since $\Delta x^k = |x^{k+1} - x^k|$ is small, $\bar{g}_l(x, x^k)$ can provide relative accurate approximation for $g_l(x)$ in k-th iteration. Note that constraint violation will be eliminated by the growing penalty parameter ρ^k.

2) The value of the exact penalty parameter ρ_M^* can hardly be determined in advance. In fact, we do not need its exact value. We can prudently choose a relatively large value for ρ_M. According to our experience, Algorithm 2 will converge even when ρ^k is much smaller than ρ_M. One reason is that $\text{Gap}_r(x^k) = \sum_l r_{ij}^l \epsilon_l^k / 4$ is actually quantified by ϵ^k. According to the previous analysis, ϵ^k is generally strictly smaller than s^k, and thus the convergence criterion could be met before all slack variables go to 0. In such circumstance, little can be said on the monotonicity of the optimal value sequence v^k. Experimental results suggest that $\{F(x^k)\}_k$ will be increasing and $\{\text{Gap}_r(x^k)\}_k$ will be decreasing. However, rigorous mathematical proof is non-trivial, because the feasible region of (15) which depends on x^k changes in every iteration, which is different from the situation in traditional penalty function theory.
3) Failure of convergence may occur in two cases: a) When the original OPF problem (5) is infeasible. In such a situation, the exact penalty parameter ρ_M^* does not exist, and FRP would not return a feasible solution. b) If the initial relaxation is very poor or an arbitrary initiation is used. In such circumstance, Algorithm 2 may converge very slowly. Possible remedy would be using valid inequalities [11], [25] to strengthen the initial relaxation.
4) In theory, CCP needs an initial point to perform linear approximation in (14). In Algorithm 2, the initial value is offered by OPF-Cr (12). In this regard, CCP-OPF makes no reference to any heuristic initial guess.

D. An Extension for Meshed Networks

OPF over meshed networks can be formulated via BIM, and come down to a non-convex quadratically constrained quadratic program, in which decision variable x consists of real and imaginary parts of complex bus voltages in rectangle coordinates. By introducing a rank-1 matrix variable $X = xx^T$, all quadratic terms can be linearized. An equivalent condition without variable x is $X \succeq 0$, $\text{rank}(X) = 1$. More details on the SDP formulation and transformation can be found in [10]. A natural way to convexify the model is to drop constraint $\text{rank}(X) = 1$, and solve a traditional SDP. At the optimal solution X^*, if $\text{rank}(X^*) = 1$ is naturally met, the relaxation is said to be exact; otherwise, the optimal value of relaxed problem provides a strict lower bound for the objective value. SDP relaxation method is well acknowledged for its ability to offer an exact convex relaxation or a high-quality optimum estimation for many practical OPF instances [27]. Nevertheless, in an inexact case, how to recover a feasible rank-1 solution remains an open problem. Some literature proposes to add rank related penalty terms in the objective function [26]–[28]. Numeric results show that when the penalty parameter resides in a proper interval, these rank penalty methods can recover a global OPF solution.

To build a connection between the SDP method and CCP-OPF method, we investigate a DC formulation for the matrix rank-1 constraint. Consider the rank-1 factorization $X = xx^T$ in an element-wise form

$$X_{ij} = x_i x_j, \ \forall i, j$$

resulting in

$$X_{ij} X_{ji} = x_i^2 x_j^2 = X_{ij}^2 = X_{ii} X_{jj}, \ \forall i, j$$

The last equality can be replaced by opposite inequalities

$$X_{ij}^2 \leq X_{ii} X_{jj}, \ \forall i, j$$

$$X_{ij}^2 \geq X_{ii} X_{jj}, \ \forall i, j$$

The former constraint is redundant to the positive semidefinite constraint $X \succeq 0$. The latter one is in fact a DC inequality in the form of $f_{ij}^1(X) - f_{ij}^2(X) \leq 0$, $\forall i, j$, where convex functions $f_{ij}^1(X)$ and $f_{ij}^2(X)$ are defined as

$$f_{ij}^1(X) = (X_{ii} + X_{jj})^2, \ \forall i, j$$

$$f_{ij}^2(X) = (X_{ii} - X_{jj})^2 + 4X_{ij}^2, \ \forall i, j$$

These constraints can be handled by a CCP framework similar to that presented in Section II.C. In case the rank penalty methods in [26]–[28] fail to offer a rank-1 solution, it is worth trying above DC formulation and CCP based method in order to recover a feasible solution. However, it should be pointed out that CCP requires solving SDPs repeatedly, which may be less efficient for large-scale systems, in spite of potential acceleration techniques enabled by exploiting the special sparsity pattern revealed in [46]. Nonetheless, these discussions may encourage new research that will leverage the computation superiority of convex optimization by exploring more appropriate DC formulation for the non-convex rank-1 constraint.

The CCP-OPF framework may be applied in two alternative OPF formulations for meshed networks. One is the extended conic quadratic model developed in [47]–[49], in which power flow equations in bus-injection format are converted to linear equalities, rotated conic quadratic equalities, and arctangent equalities via variable transformation; another one is the cycle-based model proposed in [11], where arctangent equalities in the extended conic quadratic model are replaced by cycling polynomials. If an appropriate DC decomposition for the non-convex arctangent function or the cycling polynomial is available, CCP-OPF method can be used for solving OPF of meshed networks.

Certainly, BIM and SDP based approaches can be applied to radial networks as well. The reason for the adoption of more dedicated BFM and SOCP based iterative approach is explained as follows.

1) Model comparison. BIM formulates complex bus voltages in rectangle coordinates. Line power flows are expressed as quadratic functions in real and imaginary parts of bus voltages. It is valid for both meshed and radial networks. BFM directly handles bus voltage magnitude and line power flows, and thus is more straight forward for distribution networks and system monitoring, because all variables are measurable (voltage angle and its real/imaginary part are difficult to measure due to the lack of phasor measurement units in low voltage distribution networks). Such a formulation is also convenient to be embedded in more dedicated applications in DNs, such as robust generation dispatch [50]–[52], because voltage and line flow security limits are merely bound constraints of decision variables, and the robust counterpart can be easily derived. In this regard, we employ BFM in this paper. BFM may encounter problems to model a meshed network. Since it neglects phase angle variables, the solution from BFM might give infeasible phase angles, especially on circles. For OPF problems over weakly meshed networks, the circle can be split at certain buses to make the network radial. A compensation based method is proposed in [53] to recover a solution with equal flow injections (but opposite in signs) at breakpoints, which is equivalent to the original OPF problem.
2) Algorithm comparison. The rank penalty methods discussed in [26]–[28] are non-iterative. Solving large-scale SDPs repeatedly may not be efficient. In analog to the penalty methods in [26]–[28] which append rank related terms in their objective functions, FRP in Algorithm 2 incorporates a special penalty term in the OPF objective function, which closely pertains to the relaxation gap and is updated in each iteration. The relaxation gap tends to zero when the algorithm converges. Because large-scale SOCPs can be solved efficiently via interior point methods [37], and the initial SOCP model is often nearly tight, the computational efficiency of Algorithm 2 is usually satisfactory. In conclusion, the rank penalty method in [26]–[28] and CCP-OPF method in this paper may not be able to dominate each other in terms of computational efficiency and solution quality, but the latter may be more dedicated for radial networks.
3) Finally, the proposed method can cope with non-convex objective functions [36], because any twice-differentiable function is DC representable [54]. In a similar manner, the concave part will be linearized and updated in each iteration. However, DC representation of a given function is not unique, and will significantly affect the convergence rate [55]. The optimal DC formulation that leads to the best computation performance remains an open problem, and deserves further study.

E. Case Studies

In this subsection, CCP-OPF is applied to a 6-bus system, whose topology and line data are given in Fig. 2. Generator data is provided in Table I, $p_i^n = 0$, $q_i^n = -q_i^m, \forall i \in B$. Active and reactive nodal power demands are $p_i^d = 0.6$, $q_i^d = 0.2$, $\forall i \in B$. Voltage magnitude limits are $U_i^n = 0.90$, $U_i^m = 1.05$, $U_0 = 1.05$. Parameters and test results are given in p.u.. All experiments are carried out on a laptop with Intel i5-3210M CPU and 4 GB memory. Optimization problems are coded in MATLAB with YALMIP toolbox [56]. SOCPs are solved by MOSEK [57]. This section is devoted to validating the performance of CCP-OPF, in term of convergence rate and solution quality, when the initial SOCP relaxation is not exact. The scalability and efficiency of CCP-OPF will be demonstrated on practically sized power systems in Section III and Section IV. A main consideration is that it is usually more difficult to recover a feasible/optimal solution in the forthcoming two variants of OPF problems. In all tests, Algorithm 2 converges and the solution is already very close to the global optimal one. To highlight this feature, ORP is not deployed.

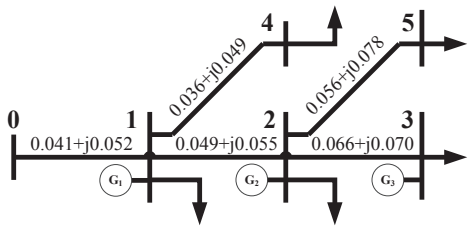

Fig. 2. Topology of the 6-bus system.

TABLE I
PARAMETERS OF GENERATORS (IN P.U.)

Unit	a_i^p	b_i^p	p_i^m	q_i^m
G_1	1.58	7.62	1.5	1.0
G_2	2.13	6.10	1.5	0.5
G_3	1.09	8.85	1.5	0.5

Case 1: The objective is to minimize the production cost F_C defined in (6). Three scenarios are under investigation. In scenario i, $i = 1, 2, 3$, only the cost parameters a_i and b_i take values in accordance with those in Table I, and others are intentionally set to 0. In this way, the objective F_C is not strictly increasing in every p_i^g. This situation is not contrived, because distributed renewable generation units, which are not rare in active DNs, usually have zero marginal production cost. Given penalty parameters $\rho^1 = 10^{-3}$, $\tau = 2$, and convergence tolerance $\varepsilon = 10^{-6}$ in Algorithm 2, results are provided in Table II. The second column is the initial relaxation gap $\text{Gap}_r(x^0)$. We can see that SOCP relaxations in the former two scenarios are inexact. FRP closes the relaxation gap within the pre-specified threshold in one or two iterations. In all three scenarios, FRP identifies the global optimal solution, which is verified by comparing the optimal values with those of (5) reported by BARON [58], a global optimization solver for NLPs using spatial branch-and-bound algorithm.

Case 2: All generator cost data takes value as that shown in Table I. The objective is to minimize the weighted-sum of production cost and voltage profile, i.e.,

$$F(x) = \lambda F_C(x) + (1 - \lambda) F_V(x) \tag{19}$$

TABLE II
PERFORMANCE OF CCP-OPF IN CASE 1

Scen.	$\text{Gap}_r(x^0)$	$\text{Gap}_r(x^k)$	Iter.	F_C	BARON
1	0.0712	4.92×10^{-7}	2	10.015	10.015
2	0.0382	1.45×10^{-7}	1	7.3265	7.3265
3	4.26×10^{-9}	4.26×10^{-9}	0	0.5321	0.5321

TABLE III
PERFORMANCE OF CCP-OPF IN CASE 2 WITH $\rho^1 = 10^{-3}$

λ (10^{-4})	$\text{Gap}_r(x^0)$	$\text{Gap}_r(x^k)$	Δx^k
0	0.0576	1.67×10^{-8}	1.9340
0.5	0.0280	4.87×10^{-9}	3.1460
1.0	0.0259	4.29×10^{-9}	3.0868
1.5	0.0238	3.98×10^{-9}	3.0296
2.0	0.0217	3.93×10^{-9}	2.9730
2.5	0.0038	9.29×10^{-9}	2.4228
3.0	0.00001	4.78×10^{-8}	2.2933

TABLE IV
OPTIMALITY GAP IN CASE 2 WITH $\rho^1 = 10^{-3}$

λ (10^{-4})	$F(x^*)$	BARON	Gap_F
0	0.0078	0.0077	1.29%
0.5	0.0093	0.0090	3.33%
1.0	0.0106	0.0104	1.92%
1.5	0.0120	0.0117	2.48%
2.0	0.0134	0.0130	3.07%
2.5	0.0148	0.0144	2.78%
3.0	0.0161	0.0157	2.49%

TABLE V
PERFORMANCE OF CCP-OPF IN CASE 2 WITH OTHER ρ^1

λ	$\rho^1 = 10^{-4}$			$\rho^1 = 10^{-5}$		
10^{-4}	Iter.	$F(x^*)$	Δx^k	Iter.	$F(x^*)$	Δx^k
0	1	0.0077	1.6450	4	0.0077	0.0192
0.5	1	0.0090	2.6629	4	0.0090	0.1922
1.0	1	0.0104	2.4598	3	0.0104	0.4348
1.5	2	0.0118	0.2934	3	0.0117	0.4220
2.0	1	0.0131	2.1223	3	0.0130	0.4778
2.5	1	0.0145	1.4825	3	0.0144	0.4784
3.0	1	0.0158	1.2767	2	0.0157	0.2439

where $F_C(x)$ is defined in (6), and $F_V(x)$ is defined in (7), the voltage reference values are selected as $U_i^r = 1.00$, $\forall i \in B$. The problem considered in this case is closely related to the BO-OPF problem discussed in Section IV. Let $\rho^1 = 10^{-3}$, $\tau = 2$, and change the weight parameter λ from 0 to 3.0×10^{-4}. Results are provided in Tables III-V.

Because F_V is not strictly monotonic, SOCP relaxation is inexact when $\lambda \leq 3 \times 10^{-4}$. FRP closes the gap within one iterations in all cases, and identifies a feasible power flow solution. To examine the solution quality, the optimal values offered by BARON and CCP-OPF are compared in Table IV. We can observe that when $\rho^1 = 10^{-3}$, the optimal values $F(x^*)$ offered by FRP are slightly higher than those $F(x^B)$ offered by BARON, the optimality gap

$$\text{Gap}_F = \frac{F(x^*) - F(x^B)}{F(x^B)} \times 100\% \tag{20}$$

shown in the last column of Table IV varies from 1% to 3%. This is because the changes in optimal solutions $\Delta x^k = |x^k - x^{k-1}|$ shown in the last column of Table III are relatively large, thus the linear approximation $\bar{g}(x, x^k)$ is not accurate enough.

We further reduce the value of ρ^1 and investigate the performance of FRP again. Results are shown in Table V. We can see that when a smaller ρ^1 is adopted, the optimal value declines to those provided by BARON, Δx^k in the last iteration decreases as well, while the number of iterations increases at the same time. In view of this, there should be a compromise between optimality and efficiency. In this case, $\rho^1 = 10^{-4}$ seems to be a good choice. Computation time is not provided in this case because the system is small, but will be elucidated in the subsequent sections.

When $\lambda = 0$ and $\rho^1 = 10^{-5}$, the values of relaxation gap $\text{Gap}_r(x^k)$ defined in (13), optimality gap $\text{Gap}_F(x^k)$ defined in (20), and objective function $F(x^k)$ defined in (19) generated in FRP are plotted in Fig. 3, showing that the two gaps decrease to 0, and the objective value approaches the global optimum.

When $\lambda > 3.1 \times 10^{-4}$, the SOCP relaxation is exact, and the optimal value does not change with respect to λ. In fact, when λ varies from 0 to 3.1×10^{-4}, the optimal solutions constitute the Pareto front of a BO-OPF problem with F_C and F_V being the objectives. However, it is not easy to derive a convincing λ because F_C and F_V exhibit different orders of magnitudes. In Section IV, we propose a non-parametric model for BO-OPF problems, which can overcome this difficulty.

Case 3: The 2-bus system in [59] is studied to illustrate the

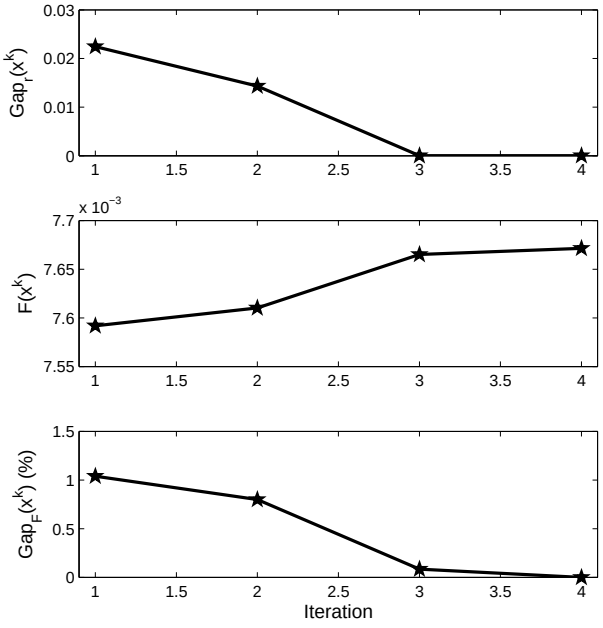

Fig. 3. Convergence performance of FRP when $\lambda = 0$ and $\rho^1 = 10^{-5}$.

performance of the SDP based CCP-OPF framework suggested in Section II.D. It is well-known that the SDP relaxation is not exact for this system when the voltage upper bound parameter $V_2^m \in [0.98, 1.03]$, although the system is not meshed in topology. The exact global optimums offered by BARON are shown in the last column of Table VI. Results of the traditional SDP relaxation are listed in the second column, showing an increasing optimality gap with growing V_2^m. We deploy an iterative method similar to Algorithm 2 with $\rho^1 = 200$ and $\tau = 1.5$. It successfully recovers the global OPF solution after a few number of iterations. When $V_2^m = 0.989$, the vector $\varsigma(X)$ which consists of singular values of the optimal solution X in each iteration is provided in Table VII. Since $\text{rank}(X)$ is equal to the number of non-zero elements in $\varsigma(X)$, the initial SDP relaxation gives a rank-3 solution, and the final optimal solution is indeed rank-1. It is also observed that when the initial SDP relaxation becomes weaker, more iterations are needed to recover a rank-1 solution.

TABLE VI
COMPUTATION PERFORMANCE WITH $\rho^1 = 200, \tau = 1.5$

V_2^m	SDP-CCP			BARON
	Obj-0	Obj-n	Iter.	
0.976	905.76	905.76	0	905.76
0.983	903.12	905.73	3	905.73
0.989	900.84	905.73	4	905.73
0.996	898.17	905.73	7	905.73
1.002	895.86	905.73	12	905.73

TABLE VII
$\varsigma(X)$ IN EACH ITERATION WHEN $V_2^m = 0.989$

Iter. 0	Iter. 1	Iter. 2	Iter. 3	Iter. 4
1.8783	1.8794	1.8763	1.8675	1.8552
0.0020	0.0012	0.0011	0.0007	0.0000
0.0003	0.0000	0.0000	0.0000	0.0000
0.0000	0.0000	0.0000	0.0000	0.0000

III. MAXIMUM LOADABILITY PROBLEM

A. Brief Introduction

Loadability refers to the ability of power systems to maintain a feasible power flow status and reliable power delivery when the demand varies. Insolvability of power flow equation is closely related to voltage instability, which is one of the major threats to a secure operation of DNs.

Traditional approaches for calculating MLA or voltage stability margin can be categorized into continuation based ones and optimization based ones. The former methods solve power flow equations repeatedly along a load increasing direction till a bifurcation point is found, such as those in [60]–[62]. The latter ones directly solve an optimization problem which maximizes the distance from a certain operating point to the boundary of power flow insolvability, such as those in [63], [64]. It is pointed out in [64] that optimization based approaches are more flexible in modeling various regulation measures and operating constraints, and could usually be more effective than continuation based ones for MLA calculation.

Although existing techniques for MLA problem are mature and tractable for large-scale instances, they may encounter challenges in determining a proper initial point that satisfies all network and equipment operating constraints, which may be difficult to acquire when an initial feasible power flow point is not clear. In addition, continuation approach needs special treatment for updating the search step around the bifurcation point. NLP based optimization approach may not be very robust due to the non-convexity of power flow equations.

To overcome these difficulties, an SDP relaxation based model and an SOCP relaxation based model are investigated in [31] and [32], respectively, for detecting power flow insolvability. SDP and SOCP belong to the category of convex optimization, and can be solved efficiently and reliably. In general, these two models can estimate an upper bound on the loadability margin without the need of a manually supplied start point. Unfortunately, although the exactness of SDP and SOCP relaxations can be guaranteed in cost-minimum OPF problems under some technical conditions, MLA application may fail to meet those conditions [31], [32], as a result, the outcome offered by these convex relaxation models can be over optimistic.

Motivated by [31], [32], this paper proposes a convex optimization based approach to compute loadability margin of radial networks, which is formulated as a special OPF problem, which can be solved by CCP-OPF. Different from SDP and SOCP relaxation models in [31] and [32], CCP-OPF outcomes an exact loadability margin.

B. Mathematical Formulation

With notations defined in Nomenclature and problem (5), MLA problem of radial networks can be expressed as a special OPF problem as follows

$$\begin{aligned} \max_{x,\eta} \quad & \eta \\ \text{s.t.} \quad & \text{Cons-PF, Cons-BD} \\ & p^d = p^{d0} + \eta \Delta p \\ & q^d = q^{d0} + \eta \Delta q \end{aligned} \tag{21}$$

where active (reactive) power demands p^{d0} (q^{d0}) correspond to a certain load scenario; Δp and Δq represent load incremental directions. Such parameter should be specified by the system operator.

Problem (21) is a variant of OPF problem (5). Because the objective function fails to meet conditions in [12] which ensure a tight SOCP relaxation for radial networks, CCP-OPF is applied to solve problem (21), and the exact loadability margin will be recovered.

As a straightforward application of the proposed CCP-OPF method, we are not aiming to develop a comprehensive model that captures every detail in voltage stability or continuation power flow calculation. In case of need, we recommend some relevant literature which addresses such modeling issues.

Generators are treated as ideal voltage sources in [31]. To consider reactive power limits of generators, complementarity constraints are proposed in [64] to model the logic of bus type switching. On-load tap changers and shunt capacitors are

TABLE VIII
COMPUTATION PERFORMANCE OF CCP-OPF

System	η	Gap$_r(x^k)$	Iter.	Time (s)
DTN-6	3.1488	4.27×10^{-9}	1	0.44
DTN-14	0.5265	2.31×10^{-8}	4	0.63
DTN-30	1.5586	1.64×10^{-8}	1	0.85
DTN-33	4.1115	5.88×10^{-7}	3	1.16
DTN-57	3.1545	3.65×10^{-7}	3	1.55
DTN-69	4.1737	1.75×10^{-7}	9	6.03
DTN-123	2.4532	2.73×10^{-10}	1	2.04
DTN-861	7.9859	4.04×10^{-7}	2	28.3

TABLE IX
COMPUTATION PERFORMANCES OF NLP SOLVERS

System	BARON		KNITRO	
	η	Time (s)	η	Time (s)
DTN-6	3.1488	3.72	3.1488	1.52
DTN-14	0.5265	14.9	0.5265	1.42
DTN-30	–	–	fail	fail
DTN-33	4.1114	332	4.1115	2.40
DTN-57	–	–	3.1545	2.56
DTN-69	–	–	fail	fail
DTN-123	–	–	2.4532	8.32
DTN-861	–	–	fail	fail

important voltage regulation equipments in DNs. Dedicated BFM with these components can be found in [52], and the corresponding problem will give rise to a mixed-integer SOCP, which is supported by many commercial solvers, such as CPLEX, GUROBI, and MOSEK.

C. Case Studies

Besides the 6-bus system, several practically-sized distribution systems are tested in this section. The data sets are available at http://shgl.curent.utk.edu/toolsdemo as well as https://sites.google.com/site/burakkocuk/research. The computation environment is the same as that in Section II.E. All testing systems are named in the form of "DTN-X" where X is the number of buses, for example, DTN-6 refers to the previous 6-bus system. In MLA problems, the nodal active and reactive power demands are chosen as $p^d = \eta p^{d0}$, $q^d = \eta q^{d0}$, where p^{d0} and q^{d0} are constants given by system load data, and η is the loadability index. Parameters of Algorithm 2 are chosen as $\rho^1 = 10^{-4}$, $\tau = 2$, and $\varepsilon = 10^{-6}$. To compare CCP-OPF with NLP solvers, problem (21) is also solved by KNITRO [65] and BARON. Results are provided in Table VIII and Table IX.

We can observe that KNITRO fails to solve MLA problem (21) associated with DTN-30, DTN-69, and DTN-861, while BARON only successes in DTN-6, DTN-14, and DTN-33, due to the increasing problem sizes. In other cases, BARON does not converge within the default time limit. CCP-OPF successfully solves all instances, verifying its robustness and scalability. It is also confirmed that CCP-OPF offers consistent loadability margins with KNITRO and BARON (if both of them work well), and is more efficient. Finally, it can be seen from the number of iterations in Table VIII that SOCP relaxation performed on problem (21) is generally not exact. FRP manages to recover the feasible, and also optimal, solution in a few number of iterations.

IV. BI-OBJECTIVE OPF PROBLEM

A. Brief Introduction

Generation dispatch of power system may involve multiple objectives, such as reducing fuel cost, carbon emission, net losses, or improving stability, voltage profile, etc. In many cases, several objectives should be coordinated or compromised, giving rise to a multi-objective OPF problem. Methods for general multi-objective optimization problems can be divided into two classes. One of them procures only one Pareto solution that compromises all objectives through a scalarized model, including the goal programming method, the weighted-sum method, and the ε-constrained method, see [66], [67] for more comprehensive surveys. A common difficulty for these methods would be how to determine convincing weights or parameters for scalarization. The other provides the entire Pareto front or evenly distributed Pareto points, such as the normal boundary intersection (NBI) method [68], and evolutionary algorithms [69]. The user makes a final decision according to his own preference.

This section proposes a non-parametric scalarization model for BO-OPF problems, which can be convexified and solved by CCP-OPF. The Pareto front can be computed via CCP-OPF embedded in the ε-constraint method (with multiple values of ε) or NBI method.

B. Mathematical Formulation

With notations defined in previous sections, the BO-OPF problem can be expressed as follows

$$\begin{aligned} \min \quad & \{F_1(x), F_2(x)\} \\ \text{s.t.} \quad & \text{Cons-PF, Cons-BD} \end{aligned} \tag{22}$$

where objective functions $F_1(x)$ and $F_2(x)$ are assumed to be convex. Let x_1^* (x_2^*) denote the unilateral optimal solution if only $F_1(x)$ ($F_2(x)$) is optimized, and $F_1^n = F_1(x_1^*)$, $F_1^m = F_1(x_2^*)$, $F_2^n = F_2(x_2^*)$, $F_2^m = F_2(x_1^*)$, then a compromising solution x^* of problem (22) can be determined by solving the following optimization problem with a scalarized objective:

$$\begin{aligned} \max_x \quad & (F_1^m - F_1(x))\,(F_2^m - F_2(x)) \\ \text{s.t.} \quad & \text{Cons-PF, Cons-BD} \end{aligned} \tag{23}$$

Its optimal solution x^* has two attractive properties:

1) x^* keeps invariant even if either objective is multiplied by a positive scalar.
2) x^* is non-dominated (Pareto optimal).

The first property is clear. For example, if $F_1(x)$ becomes $\sigma F_1(x)$, where $\sigma > 0$ is a constant, then both F_1^m and the objective of (23) will be multiplied by σ, and the optimal solution remains the same. This property implies that x^* is independent of the relative ratio between the two objectives.

To see the second one, suppose x^* is not a Pareto solution, and can be dominated by x^{**}, then it must satisfy $F_1(x^{**}) \leq$

$F_1(x^*)$, $F_2(x^{**}) \leq F_2(x^*)$, and at least one of them holds as a strict inequality, so the objective value at x^{**} is greater than that at x^*, which is in contradiction with the assumption that x^* is an optimal solution of (23).

To convexify the objective function, we introduce axillary variables t_1, t_2, and t_b, then build the problem

$$\begin{aligned} &\max_{x,t} \quad t_b \\ s.t.\ &\text{Cons-PF, Cons-BD} \\ &t_1 \leq F_1^m - F_1(x) \\ &t_2 \leq F_2^m - F_2(x) \\ &t_1 \geq 0,\ t_2 \geq 0,\ t_1 t_2 \geq t_b^2 \end{aligned} \tag{24}$$

Problem (24) and problem (23) share the same optimal solution in variable x, and $\sqrt{(F_1^m - F_1(x^*))(F_2^m - F_2(x^*))} = t_b^*$ holds at optimum. The last hyperbolic inequality of (24) can be replaced with an SOC inequality

$$\left\| \begin{matrix} 2t_b \\ t_1 - t_2 \end{matrix} \right\| \leq t_1 + t_2$$

Because $F_1(x)$ and $F_2(x)$ are convex, the only non-convexity rests in (4) of Cons-PF. In this regard, problem (24) is another variant of OPF problem (5), and can be solved by CCP-OPF.

If the goal of BO-OPF problem is to find a set of uniformly distributed Pareto points, rather than only one compromising solution, the ε-constraint method and NBI method will be good choices for this task. The former approach solves the following problem with some values of ε that are delicately sampled from interval $[F_2^l, F_2^m]$

$$\min\ \{F_1(x) : \text{Cons-PF, Cons-BD},\ F_2(x) \leq \varepsilon\} \tag{25}$$

The last inequality is convex. Problem (25) with given ε is similar to problem (5), and can be solved by CCP-OPF.

The NBI method has been applied to the multi-objective OPF problem in NLP form in [70]. The bi-objective case is elucidated in Fig. 4. Two extreme points of Pareto front are

$$\Phi_1 = \begin{bmatrix} F_1(x_1^*) \\ F_2(x_1^*) \end{bmatrix},\ \Phi_2 = \begin{bmatrix} F_1(x_2^*) \\ F_2(x_2^*) \end{bmatrix}$$

Define matrix $\Phi = [\Phi_1, \Phi_2]$, then any point on line segment L_F^S connecting Φ_1 and Φ_2 can be expressed via

$$P(\beta) = \Phi\beta,\ \beta = [\beta_1, \beta_2],\ 0 \leq \beta_1, \beta_2 \leq 1,\ \beta_1 + \beta_2 = 1$$

where parameter β controls the location of point $P(\beta)$.

Let $\vec{n}$ be a unit vector that is perpendicular to L_F^S, which can be calculated as

$$\vec{n} = \frac{-[\Delta F_1, \Delta F_2]^T}{\sqrt{\Delta F_1^2 + \Delta F_2^2}}$$

where $\Delta F_1 = F_1^m - F_1^n > 0$, $\Delta F_2 = F_2^m - F_2^n > 0$.

Provided with well-distributed initiating points $P(\beta_m)$, $m = 1, 2, \cdots, M$ on L_F^S, the key step performed in NBI method is to detect a Pareto point on line $L_{P(\beta_m)}^{\vec{n}}$ which passes through

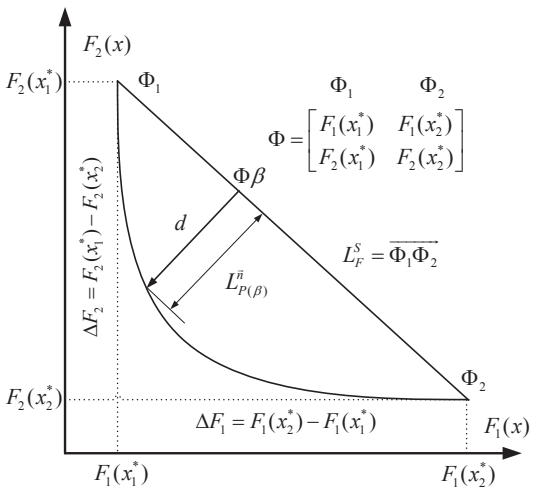

Fig. 4. Illustration of NBI method.

point $P(\beta_m)$ and is orthogonal to L_F^S. This task can be implemented by solving the following problem [68], [70]

$$\begin{aligned} &\max_{x,d} \quad d \\ &s.t.\ \text{Cons-PF, Cons-BD} \\ &\Phi\beta_m + d\vec{n} = \begin{bmatrix} F_1(x) \\ F_2(x) \end{bmatrix} \end{aligned} \tag{26}$$

If both $F_1(x)$ and $F_2(x)$ are linear, the last constraint is also linear. The Pareto point detection problem (26) is similar to MLA problem (21), and the optimal solution x_m^* can be solved by OPF-CCP. The set of points $[F_1(x_m^*), F_2(x_m^*)]^T$, $m = 1, 2, \cdots$ are almost evenly distributed on the Pareto front. The last equality can be relaxed as convex inequality

$$\Phi\beta_m + d\vec{n} \geq \begin{bmatrix} F_1(x) \\ F_2(x) \end{bmatrix}$$

when $F_1(x)$ and $F_2(x)$ are nonlinear but convex functions, where "$\geq$" means element-wise "greater than or equal to".

C. Case Studies

Testing systems in Section III.C are used again for studying the BO-OPF problem. Production cost $F_C(x)$ and voltage profile $F_V(x)$ are considered for optimization. The computation environment is the same as that in Section II.E. Bound parameters F_C^l, F_C^m, F_V^l, and F_V^m of both objective functions are computed using CCP-OPF, and shown in Table X. The base value of cost is \$1000.

The BO-OPF problem associated with DTN-6 is studied first. The Pareto front is computed by using the ε-constraint method, and shown in Fig. 5. The trade-off solution retrieved from problem (24) is plotted in the same figure, located in the "middle" of Pareto front without a manually supplied parameter or particular normalization process. This is an attractive feature because different objectives in a BO-OPF problem usually exhibit different orders of magnitudes.

Results of remaining systems are shown in Tables XI-XIII, where x_b^* is the tradeoff solution computed from (24),

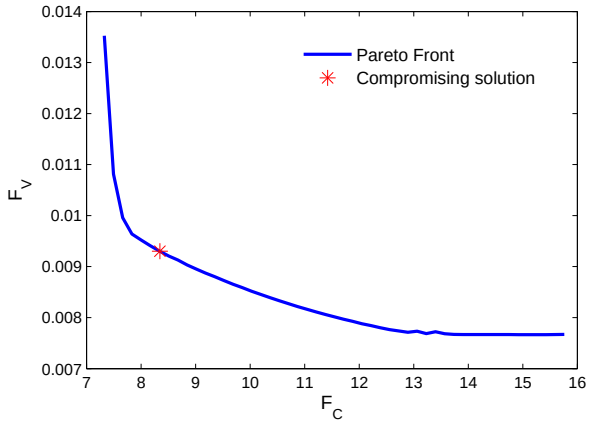

Fig. 5. Pareto front and compromising solution of the 6-bus system.

TABLE X
BOUND PARAMETERS OF F_C AND F_V

System	F_C^l	F_C^m	F_V^l	F_V^m
DTN-6	7.3265	15.8204	0.0077	0.0137
DTN-14	8.7638	10.328	0.0280	0.0745
DTN-30	11.785	13.685	0.0984	0.5950
DTN-33	35.5128	36.4881	0.2710	0.4379
DTN-57	12.410	13.860	0.0231	0.0535
DTN-69	46.2022	49.8723	0.3356	0.7408
DTN-123	24.9816	26.2172	0.1647	0.4568
DTN-861	26.3904	87.3602	0.9971	3.1522

$B_V(x_b^*) = [F_C^m - F_C(x_b^*)][F_V^m - F_V(x_b^*)]$ is the optimal value of (23). CCP-OPF is applied to solve these BO-OPF problems in form of (24), and successes in all instances within a few number of iterations. The computation time for DTN-861 is a little bit longer, but still acceptable. For NLP solvers, BARON manages to solve most of these BO-OPF problems, as for DTN-861, it fails to converge within the default time limit. Results shown in Table XI and Table XII corroborate that those solutions offered by CCP-OPF are indeed very close to the global optimal ones. Nevertheless, CCP-OPF is much more efficient. We find that KNITRO is not robust in solving BO-OPF problems, and switch to IPOPT [71], which is implemented based on the primal-dual interior point method. The same instances are solved again. Results are provided in Table XIII. In these tests, IPOPT fails in problems of DTN-69 and DTN-861, and does not offer an (local) optimal solution for DTN-57 with default settings. Other results are consistent with those of CCP and BARON. Although the computational efficiency of IPOPT is comparable with CCP-OPF, especially for medium-scale systems, the latter appears to be more robust, because it only involves solving SOCPs.

V. CONCLUSIONS

This paper provides important supplementary materials for the emerging convex relaxation methods of the OPF problem, a fundamental issue in power system steady-state operation. The BFM based formulation exhibits a special structure of

TABLE XI
BI-OBJECTIVE OPF RESULTS OFFERED BY OPF-CCP

System	Iter	Time(s)	$F_C(x_b^*)$	$F_V(x_b^*)$	$B_V(x_b^*)$
DTN-6	3	0.34	8.3540	0.0093	0.0326
DTN-14	7	2.79	9.2468	0.0377	0.0436
DTN-30	1	1.12	12.369	0.2687	0.4294
DTN-33	1	0.99	35.8610	0.3137	0.0779
DTN-57	5	8.41	13.021	0.0361	0.0146
DTN-69	2	1.34	46.9372	0.3664	1.0988
DTN-123	3	8.77	25.3540	0.2492	0.1792
DTN-861	9	98.7	26.8086	1.3582	108.63

TABLE XII
BI-OBJECTIVE OPF RESULTS OFFERED BY BARON

System	$F_C^b(x_b^*)$	$F_V^b(x_b^*)$	$B_V(x_b^*)$	Time(s)
DTN-6	8.3174	0.0093	0.0329	239
DTN-14	9.2470	0.0377	0.0436	12
DTN-30	12.369	0.2686	0.4295	57
DTN-33	35.8617	0.3136	0.0779	114
DTN-57	13.021	0.0361	0.0146	132
DTN-69	46.9341	0.3668	1.0988	170
DTN-123	25.3545	0.2485	0.1797	66
DTN-861	–	–	–	–

TABLE XIII
BI-OBJECTIVE OPF RESULTS OFFERED BY IPOPT

System	$F_C^b(x_b^*)$	$F_V^b(x_b^*)$	$B_V(x_b^*)$	Time(s)
DTN-6	8.3645	0.0093	0.0329	3.02
DTN-14	9.2465	0.0377	0.0436	2.71
DTN-30	12.368	0.2688	0.4295	1.64
DTN-33	35.8609	0.3137	0.0779	2.26
DTN-57	non-opt	non-opt	non-opt	non-opt
DTN-69	fail	fail	fail	fail
DTN-123	25.3541	0.2486	0.1797	7.32
DTN-861	fail	fail	fail	fail

DCP, and can be solved by CCP-OPF, a sequential SOCP procedure. It makes no reference to a heuristic initial guess desired by local NLP algorithms, and removes the need of an exactness guarantee required by existing convex relaxation methods, while leveraging the computational superiority of convex optimization. Two variants of OPF problems discussed in this paper cover several classical issues in power generation dispatch. In these regards, the proposed computation framework greatly enhances our ability to solve broader classes of OPF problems, and may become a promising computational tool for power system analysis, due to the elementary role of OPF. For example, it would be useful in distribution market studies, such as electricity pricing and strategic bidding, because calculating distribution locational marginal prices, the Lagrangian dual multipliers associated with nodal active power balancing equalities, relies on an OPF solution.

ACKNOWLEDGMENT

The authors appreciate the insightful comments and valuable suggestions offered by the anonymous reviewers, which help improve the quality of this paper significantly. The first author would like to thank Prof. Steven H. Low at California Institute of Technology for his helpful discussions on the early version of this paper.

REFERENCES

[1] H. W. Dommel and W. Tinney, "Optimal power flow solutions," *IEEE Trans. Power App. Syst.*, vol. 87, no. 10, pp. 1866–1876, Oct. 1968.

[2] M. E. Baran and F. F. Wu, "Network reconfiguration in distribution systems for loss reduction and load balancing," *IEEE Trans. Power Del.*, vol. 4, no. 2, pp. 1401–1407, Apr. 1989.

[3] ——, "Optimal capacitor placement on radial distribution systems," *IEEE Trans. Power Del.*, vol. 4, no. 1, pp. 725–734, Jan. 1989.

[4] ——, "Optimal sizing of capacitors placed on a radial distribution system," *IEEE Trans. Power Del.*, vol. 4, no. 1, pp. 735–743, Jan. 1989.

[5] J. A. Momoh, M. E. El-Hawary, and R. Adapa, "A review of selected optimal power flow literature to 1993. Part I: Nonlinear and quadratic programming approaches," *IEEE Trans. Power Syst.*, vol. 14, no. 1, pp. 96–104, Feb. 1999.

[6] ——, "A review of selected optimal power flow literature to 1993. Part II: Newton, linear programming and interior point methods," *IEEE Trans. Power Syst.*, vol. 14, no. 1, pp. 105–111, Feb. 1999.

[7] S. Frank, I. Steponavice, and S. Rebennack, "Optimal power flow: a bibliographic survey, I: formulations and deterministic methods," *Energy Systems*, vol. 3, no. 3, pp. 221–258, Sep. 2012.

[8] ——, "Optimal power flow: a bibliographic survey, II: nondeterministic and hybrid methods," *Energy Systems*, vol. 3, no. 3, pp. 259–289, Sep. 2012.

[9] X. Bai, H. Wei, K. Fujisawa, and Y. Wang, "Semidefinite programming for optimal power flow problems," *Int. J. Elec. Power*, vol. 30, no. 6-7, pp. 383–392, Jul. 2008.

[10] J. Lavaei and S. H. Low., "Zero duality gap in optimal power flow problem," *IEEE Trans. Power Syst.*, vol. 27, no. 1, pp. 92–107, Feb. 2012.

[11] B. Kocuk, S. S. Dey, and X. A. Sun, "Strong SOCP relaxations for optimal power flow," *Oper. Res.*, vol. 64, no. 6, pp. 1177–1196, May 2016.

[12] M. Farivar and S. H. Low, "Branch flow model: Relaxations and convexification," *IEEE Trans. Power Syst.*, vol. 28, no. 3, pp. 2554–2572, Aug. 2013.

[13] C. Josz, J. Maeght, P. Panciatici, and J. C. Gilbert, "Application of the moment-SOS approach to global optimization of the OPF problem," *IEEE Trans. Power Syst.*, vol. 30, no. 1, pp. 463–470, Jan. 2015.

[14] D. K. Molzahn and I. A. Hiskens, "Sparsity-exploiting moment-based relaxations of the optimal power flow problem," *IEEE Trans. Power Syst.*, vol. 30, no. 6, pp. 3168–3180, Nov. 2015.

[15] B. Ghaddar, J. Marecek, and M. Mevissen, "Optimal power flow as a polynomial optimization problem," *IEEE Trans. Power Syst.*, vol. 31, no. 1, pp. 539–546, Jan. 2016.

[16] C. Coffrin, H. L. Hijazi, and P. V. Hentenryck, "The QC relaxation: A theoretical and computational study on optimal power flow," *IEEE Trans. Power Syst.*, vol. 31, no. 4, pp. 3008–3018, 2016.

[17] S. H. Low, "Convex relaxation of optimal power flow part I: Formulations and equivalence," *IEEE Trans. Control Network Systems*, vol. 1, no. 1, pp. 15–27, Mar. 2014.

[18] ——, "Convex relaxation of optimal power flow part II: Exactness," *IEEE Trans. Control Network Systems*, vol. 1, no. 2, pp. 177–189, Jun. 2014.

[19] B. Zhang and D. Tse, "Geometry of injection regions of power networks," *IEEE Trans. Power Syst.*, vol. 28, no. 2, pp. 788–797, May 2013.

[20] J. Lavaei, D. Tse, and B. Zhang, "Geometry of power flows and optimization in distribution networks," *IEEE Trans. Power Syst.*, vol. 29, no. 2, pp. 572–583, Mar. 2014.

[21] S. Sojoudi, S. Fattahi, and J. Lavaei, "Convexification of generalized network flow problem," *Preprint*, vol. available at: http://www.ieor.berkeley.edu/lavaei/Generalized_Net_Flow.pdf.

[22] N. Li, L. Chen, and S. H. Low, "Exact convex relaxation of OPF for radial networks using branch flow model," in *Proc. IEEE Third International Conference on Smart Grid Communications*, Tainan, Nov. 2012, pp. 7–12.

[23] L. Gan, N. Li, U. Topcu, and S. H. Low, "Exact convex relaxation of optimal power flow in radial networks," *IEEE Trans. Autom. Control*, vol. 60, no. 1, pp. 72–87, Jan. 2015.

[24] S. Huang, Q. Wu, J. Wang, and H. Zhao, "A sufficient condition on convex relaxation of AC optimal power flow in distribution networks," *IEEE Trans. Power Syst.*, vol. 32, no. 2, pp. 1359–1368, Mar. 2017.

[25] B. Kocuk, S. S. Dey, and X. A. Sun, "Inexactness of SDP relaxation and valid inequalities for optimal power flow," *IEEE Trans. Power Syst.*, vol. 31, no. 1, pp. 642–651, Jan. 2016.

[26] R. Madani, M. Ashraphijuo, and J. Lavaei, "Promises of conic relaxation for contingency-constrained optimal power flow problem," *IEEE Trans. Power Syst.*, vol. 31, no. 2, pp. 1297–1307, Mar. 2016.

[27] R. Madani, S. Sojoudi, and J. Lavaei, "Convex relaxation for optimal power flow problem: Mesh networks," *IEEE Trans. Power Syst.*, vol. 30, no. 1, pp. 199–211, Jan. 2015.

[28] D. Molzahn, C. Josz, I. Hiskens, and P. Panciatici, "Solution of optimal power flow problems using moment relaxations augmented with objective function penalization," in *54th Annual Conference on Decision and Control*, Osaka, Japan, Dec. 2015, pp. 31–38.

[29] C. Chen, A. Atamtürk, and S. S. Oren, "Bound tightening for the alternating current optimal power flow problem," *IEEE Trans. Power Syst.*, vol. 31, no. 5, pp. 3729–3736, Sep. 2016.

[30] D. T. Phan, "Lagrangian duality and branch-and-bound algorithms for optimal power flow," *Oper. Res.*, vol. 60, no. 2, pp. 275–285, 2012.

[31] D. Molzahn, B. Lesieutre, and C. DeMarco, "A sufficient condition for power flow insolvability with applications to voltage stability margins," *IEEE Trans. Power Syst.*, vol. 28, no. 3, pp. 2592–2601, Aug. 2013.

[32] D. Molzahn, I. Hiskens, and B. Lesieutre., "Calculation of voltage stability margins and certification of power flow insolvability using second-order cone programming," in *49th Hawaii International Conference on System Sciences*, Kauai, Hawaii, Jan. 2016, pp. 2307–2316.

[33] T. P. Dinh and H. A. L. Thi, "Recent advances in DC programming and DCA," *Trans. Comput. Intell.*, vol. 13, pp. 1–37, 2014.

[34] H. Tuy, *Convex Analysis and Global Optimization, 2nd Edition*. Springer, 2016.

[35] P. D. Tao, "The DC (difference of convex functions) programming and DCA revisited with DC models of real world nonconvex optimization problems," *Ann. Oper. Res.*, vol. 133, no. 1, pp. 23–46, Jan. 2005.

[36] T. Lipp and S. Boyd, "Variations and extension of the convex-concave procedure," *Optim. Eng.*, vol. 17, no. 2, pp. 263–287, 2016.

[37] M. S. Lobo, L. Vandenberghe, S. Boyd, and H. Lebret, "Applications of second-order cone programming," *Linear Algebra Appl.*, vol. 284, no. 1, pp. 193–228, Nov. 1998.

[38] S. P. Han and O. L. Mangasarian, "Exact penalty functions in nonlinear programming," *Math. Program.*, vol. 17, no. 1, pp. 251–269, Dec. 1979.

[39] G. D. Pillo and L. Grippo, "Exact penalty functions in constrained optimization," *SIAM J. Control Optim.*, vol. 27, no. 6, pp. 1333–1360, 1989.

[40] H. Wei, H. Sasaki, J. Kubokawa, and R. Yokoyama, "An interior point nonlinear programming for optimal power flow problems with a novel data structure," *IEEE Trans. Power Syst.*, vol. 13, no. 3, pp. 870–877, Aug. 1998.

[41] Y. C. Wu, A. S. Debs, and R. E. Marsten, "A direct nonlinear predictor-corrector primal-dual interior point algorithm for optimal power flows," *IEEE Trans. Power Syst.*, vol. 9, no. 2, pp. 876–883, May 1994.

[42] R. A. Jabr, A. H. Coonick, and B. J. Cory, "A primal-dual interior point method for optimal power flow dispatching," *IEEE Trans. Power Syst.*, vol. 17, no. 3, pp. 654–662, Aug. 2002.

[43] G. P. Granelli and M. Montagna, "Security-constrained economic dispatch using dual quadratic programming," *Electr. Power Syst. Res.*, vol. 56, no. 1, pp. 71–80, Oct. 2000.

[44] P. T. Boggs and J. W. Tolle, "Sequential quadratic programming for large-scale nonlinear optimization," *J. Comput. Appl. Math.*, vol. 124, no. 1-2, pp. 123–137, Dec. 2000.

[45] ——, "Sequential quadratic programming," *Acta Numer.*, vol. 4, pp. 1–51, 1995.

[46] M. S. Andersen, A. Hansson, and L. Vandenberghe, "Reduced-complexity semidefinite relaxations of optimal power flow problems," *IEEE Trans. Power Syst.*, vol. 29, no. 4.

[47] A. G. Esposito and E. R. Ramos, "Reliable load flow technique for radial distribution networks," *IEEE Trans. Power Syst.*, vol. 14, no. 3, pp. 1063–1069, Aug. 1999.

[48] R. A. Jabr, "Radial distribution load flow using conic programming," *IEEE Trans. Power Syst.*, vol. 21, no. 3, pp. 1458–1459, Aug. 2006.

[49] ——, "Optimal power flow using an extended conic quadratic formulation," *IEEE Trans. Power Syst.*, vol. 23, no. 3, pp. 1000–1008, Aug. 2008.

[50] W. Wei, S. Mei, J. Wang, L. Wu, and Y. Fang, "Robust operation of distribution networks coupled with urban transportation infrastructures," *IEEE Trans. Power Syst. in press*.

[51] T. Ding, C. Li, Y. Yang, J. Jiang, Z. Bie, and F. Blaabjerg, "A two-stage robust optimization for centralized-optimal dispatch of photovoltaic inverters in active distribution networks," *IEEE Trans. Sustain. Energy in press*.

[52] T. Ding, S. Liu, W. Yuan, Z. Bie, and B. Zeng, "A two-stage robust reactive power optimization considering uncertain wind power integration in active distribution networks," *IEEE Trans. Sustain. Energy*, vol. 7, no. 1, pp. 301–311, Jan. 2016.

[53] R. A. Jabr and I. Džafić, "A compensation-based conic OPF for weakly meshed networks," *IEEE Trans. Power Syst.*, vol. 31, no. 5, pp. 4167–4168, Sep. 2016.

[54] P. Hartman, "On functions representable as a difference of convex functions," *Pac. J. Math.*, vol. 9, no. 3, pp. 707–713, Jul. 1959.

[55] T. V. Voorhisa and F. A. Al-Khayyal, "Difference of convex solution of quadratically constrained optimization problems," *Eur. J. Oper. Res.*, vol. 148, no. 2, pp. 349–362, Jul. 2003.

[56] J. Löfberg, "YALMIP: A toolbox for modeling and optimization in MATLAB," in *IEEE International Symposium on Computer Aided Control Systems Design*, Taipei, Taiwan, Sep. 2004, pp. 284–289.

[57] (2016) Mosek website. [Online]. Available: https://www.mosek.com/

[58] M. Tawarmalani and N. V. Sahinidis, "A polyhedral branch-and-cut approach to global optimization," *Math. Program.*, vol. 103, no. 2, pp. 225–249, Jun. 2005.

[59] W. A. Bukhsh, A. Grothey, K. I. M. McKinnon, and P. A. Trodden, "Local solutions of the optimal power flow problem," *IEEE Trans. Power Syst.*, vol. 28, no. 4, pp. 4780–4788, Nov. 2013.

[60] V. Ajjarapu and C. Christy, "The continuation power flow: a tool for steady state voltage stability analysis," *IEEE Trans. Power Syst.*, vol. 7, no. 1, pp. 416–423, Feb. 1992.

[61] H. D. Chiang, A. J. Flueck, K. S. Shah, and N. Balu, "CPFLOW: a practical tool for tracing power system steady-state stationary behavior due to load and generation variations," *IEEE Trans. Power Syst.*, vol. 10, no. 2, pp. 623–634, May 1995.

[62] S. H. Li and H. D. Chiang, "Nonlinear predictors and hybrid corrector for fast continuation power flow," *IET Gener. Transm. Dis.*, vol. 2, no. 3, pp. 341–354, May 2008.

[63] G. D. Irisarri, X. Wang, J. Tong, and S. Mokhtari, "Maximum loadability of power systems using interior point nonlinear optimization method," *IEEE Trans. Power Syst.*, vol. 12, no. 1, pp. 162–172, Feb. 1997.

[64] R. J. Avalos, C. A. Canizares, F. Milano, and A. J. Conejo, "Equivalency of continuation and optimization methods to determine saddle-node and limit-induced bifurcations in power systems," *IEEE Trans. Circuits-I*, vol. 56, no. 1, pp. 210–223, Jan. 2009.

[65] R. H. Byrd, J. Nocedal, and R. A. Waltz, "Knitro: An integrated package for nonlinear optimization," in *Large-Scale Nonlinear Optimization*, G. D. Pillo and M. Roma, Eds. New York, NY, USA: Springer, 2006, ch. 4, pp. 35–59.

[66] R. T. Marler and J. S. Arora, "Survey of multi-objective optimization methods for engineering," *Struct. Multidisc. Optim.*, vol. 26, no. 6, pp. 369–395, Apr. 2004.

[67] M. Caramia and P. Dell'Olmo, "Multi-objective optimization," in *Multi-objective Management in Freight Logistics*. Springer, 2008, ch. 2, pp. 11–36.

[68] I. Das and J. E. Dennis, "Normal-boundary intersection: A new method for generating the pareto surface in nonlinear multicriteria optimization problems," *SIAM J. Optim.*, vol. 8, no. 3, pp. 631–657, 1998.

[69] A. Zhou, B. Qu, H. Li, S. Zhao, P. Suganthan, and Q. Zhang, "Multiobjective evolutionary algorithms: A survey of the state of the art," *Swarm and Evolutionary Computation*, vol. 1, no. 1, pp. 32–49, Mar. 2011.

[70] C. Roman and W. Rosehart, "Evenly distributed Pareto points in multi-objective optimal power flow," *IEEE Trans. Power Syst.*, vol. 21, no. 2, pp. 1011–1012, May 2006.

[71] A. Wächter and L. T. Biegler, "On the implementation of an interior-point filter line-search algorithm for large-scale nonlinear programming," *Math. Program.*, vol. 106, no. 1, pp. 25–57, Mar. 2006.

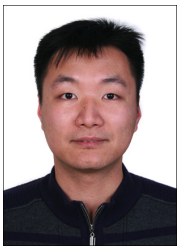

Wei Wei (M'15) received the B.Sc. and Ph.D. degrees in electrical engineering from Tsinghua University, Beijing, China, in 2008 and 2013, respectively.

He was a Postdoctoral Researcher with Tsinghua University from 2013 to 2015. He was a Visiting Scholar with Cornell University, Ithaca, NY, USA, in 2014, and with Harvard University, Cambridge, MA, USA, in 2015. He is currently an Assistant Professor with Tsinghua University. His research interests include applied optimization and energy economics.

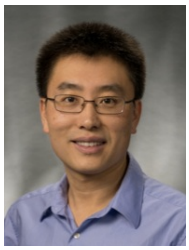

Jianhui Wang (M'07-SM'12) received the Ph.D. degree in electrical engineering from Illinois Institute of Technology, Chicago, IL, USA, in 2007.

Presently, he is an Associate Professor with the Department of Electrical Engineering at Southern Methodist University, Dallas, Texas, USA. He also holds a joint appointment as Section Lead for Advanced Power Grid Modeling at the Energy Systems Division at Argonne National Laboratory, Argonne, Illinois, USA.

Dr. Wang is the secretary of the IEEE Power & Energy Society (PES) Power System Operations, Planning & Economics Committee. He is an associate editor of Journal of Energy Engineering and an editorial board member of Applied Energy. He has held visiting positions in Europe, Australia and Hong Kong including a VELUX Visiting Professorship at the Technical University of Denmark (DTU). Dr. Wang is the Editor-in-Chief of the IEEE Transactions on Smart Grid and an IEEE PES Distinguished Lecturer. He is also the recipient of the IEEE PES Power System Operation Committee Prize Paper Award in 2015.

Na Li (M'09) received her B.S. degree in mathematics and applied mathematics from Zhejiang University in China and her PhD degree in Control and Dynamical systems from the California Institute of Technology in 2013.

She is an Assistant Professor in the School of Engineering and Applied Sciences in Harvard University. She was a postdoctoral associate of the Laboratory for Information and Decision Systems at Massachusetts Institute of Technology. She was a Best Student Paper Award finalist in the 2011 IEEE Conference on Decision and Control. Her research lies in the design, analysis, optimization and control of distributed network systems, with particular applications to power networks and systems biology/physiology.

Shengwei Mei (F'15) received the B.Sc. degree in mathematics from Xinjiang University, Urumqi, China, the M.Sc. degree in operations research from Tsinghua University, Beijing, China, and the Ph.D. degree in automatic control from Chinese Academy of Sciences, Beijing, China, in 1984, 1989, and 1996, respectively.

He is currently a Professor of Tsinghua University, Beijing, China. His research interests include power system complexity and control, game theory and its application in power systems.